Proceedings of the 20th International Conference on Soil Mechanics and Geotechnical Engineering– Rahman and Jaksa (Eds)
© 2022 Australian Geomechanics Society, Sydney, Australia, ISBN 978-0-9946261-4-1

Effect of drained cyclic preshearing on the undrained cyclic response of dense sand in triaxial tests

Effet du chargement cyclique drainée sur la réponse cyclique non drainée du sable dense avec essais triaxiaux

Pasquale Carotenuto, Hans Petter Jostad & Yining Teng
Norwegian Geotechnical Institute, Norway, pasquale.carotenuto@ngi.no

ABSTRACT: The characterization of sand response under undrained cyclic loading is of key importance for optimal design of offshore foundations and for site liquefaction assessment. Among various aspects influencing this response, this paper focuses on the effect of drained cyclic load history (*preshearing*) on the subsequent undrained cyclic behavior for a dense clean silica sand. Results from a series of cyclic undrained triaxial tests are presented, where undrained cyclic shear strength and stiffness are analyzed as function of the cyclic shear stress amplitude applied during drained cyclic preshearing. It is found that preshearing leads to small changes in relativity density (i.e. not larger than 0.2%), but that it significantly influences cyclic stiffness, strength and pore pressure build-up during the subsequent undrained cyclic loading to failure. The cyclic shear modulus, G_{cy} in the first 30 undrained load cycles is found to increase from values in the range 8-45 MPa when no preshearing is applied to values in the range 76-82 MPa when the highest preshearing is applied; the number of cycles to failure, N_f increases from 60 to 245 for the same two cases. Re-arrangement of intergranular reactions is hypothesized to be the cause of the observed preshearing effects.

RÉSUMÉ : La caractérisation de la réponse du sable sous charge cyclique non drainée est d'une importance clé pour la conception optimale des fondations offshore et pour l'évaluation de la liquéfaction du site. Parmi divers aspects influençant cette réponse, cet article se concentre sur l'effet de l'histoire de charge cyclique drainée (précisaillement) sur le comportement cyclique non drainé subséquent dans un sable de silice propre et dense. Les résultats d'une série d'essais triaxiaux cycliques non drainés sont présentés, où la résistance au cisaillement cyclique non drainé et la rigidité sont analysées en fonction de l'amplitude de la contrainte de cisaillement cyclique appliquée pendant le précisaillement cyclique drainé. On constate que le précisaillement entraîne de petits changements dans la densité de relativité (c'est-à-dire pas plus de 0,2 %), mais qu'il influence de manière significative la rigidité cyclique, la résistance et l'accumulation de pression interstitielle pendant le chargement cyclique non drainé jusqu'à la rupture. Le module de cisaillement cyclique G_{cy} dans les 30 premiers cycles de charge augmente d'une plage de 8-45 MPa pour l'essai sans précisaillement à une plage de 76-82 MPa pour l'essai avec le plus haut précisaillement ; le nombre de cycles jusqu'à rupture, N_f passe de 60 à 245 entre les deux mêmes essais. Le réarrangement des réactions intergranulaires est supposé être la cause des effets de précisaillement observés.

KEYWORDS: Sand, Cyclic loading, Preshearing, Cyclic load history

1 INTRODUCTION

Cyclic loading on sands has been the subject of extensive studies, in connection with both liquefaction problems and offshore foundations. The rapid development of the offshore wind industry in the last decade has put further focus on this topic. Sand behavior under cyclic loading is dependent on a number of factors such as soil intrinsic properties (e.g. grain size distribution, particle sphericity, angularity), current soil state (e.g. consolidation stresses and relative density Dr) and the applied cyclic loading, see for instance Andersen (2015). Another factor affecting sand behavior is cyclic load history, which is the focus of the present paper. Specific attention is given herein to the impact of drained cyclic load history on the subsequent undrained cyclic response to failure. Drained cyclic load history is referred throughout this paper as *preshearing*. The paper considers moist-tamped reconstituted sand specimens, since undisturbed sand specimens are not routinely obtained.

Seed et al. (1977) investigated the effect of preshearing on liquefaction of saturated sands by means of shaking table tests. The number of cycles to liquefaction was found to increase by a factor of 8 to 10 compared to parallel tests without preshearing. They observed that the increase of relative density due to preshearing was relatively small, in the order of less than 1%, which according to the authors could not explain the observed increase in resistance to liquefaction. Within cyclic testing on reconstituted sand specimens for offshore foundation projects, the word *preshearing* typically refers to the practice of applying small drained cyclic loading prior to undrained cyclic shearing to failure, in order to model the effect of environmental load history (Andersen, 2015). Within this practice, several hundred cycles with normalized cyclic shear stress $\tau_{cy\_pre}/\sigma'_{ac}$ about 0.04 to 0.06 are typically applied. Andersen (2015) indicates that this type of preshearing increases cyclic resistance of sands. Quinteros et al. (2017) on the other hand report that preshearing has generally small to no impact on monotonic triaxial drained and undrained soil response.

The present study systematically investigates the effects of drained cyclic preshearing on reconstituted clean silica sand specimens in the triaxial apparatus. The realm of investigation is not limited to the preshearing levels used in typical offshore practice (i.e. $\tau_{cy\_pre}/\sigma'_{ac}$ about 0.04-0.06), but it extends well beyond these values, up to 0.43.

The following definitions in relation to cyclic testing are used in this paper (Andersen, 2015). Cyclic strains and stresses within a cycle are defined as half of the difference between the maximum and minimum values within the cycle (semi-amplitude values). Permanent strains and stresses within a cycle are defined as the values at the end of the cycle. Cyclic and permanent values are indicated with the subscript *cy* and *p*, respectively.

2 LABORATORY PROGRAM AND METHODS

2.1 *Material tested*

The soil tested is a clean silica sand originally sampled from an offshore site in the Norwegian sector of the North Sea. The fractions below 0.063 mm and above 0.50 mm were removed by sieving. Material properties are given in Table 1.

Table 1. Properties of Norwegian offshore sand tested

Gs	D60	D10	Cu	$\gamma_{d,max}$	$\gamma_{d,min}$	e_{min}	e_{max}
-	mm	mm	-	kN/m^3	kN/m^3	-	-
2.70	0.186	0.099	1.88	17.14	14.29	0.85	0.54

2.2 *Laboratory program and procedures*

Six anisotropically consolidated undrained cyclic triaxial tests were carried out. Testing conditions for each test are summarized in Table 2.

Specimens were reconstituted by the moist-tamping undercompation method (Ladd, 1978), following the details described in Knudsen et al. (2019). The specimen initial height and diameter were 108 mm and 54 mm respectively (H/D = 2). The initial water content for reconstitution was 3%. The initial Dr_i ranged between 73.2% and 77.2%.

After reconstitution, specimens were flushed with CO_2 for 30 minutes, then with de-aired water for another 30 minutes, and finally a back pressure of 1.3 MPa was applied. Skempton's B-values between 97% and 98% were measured in all tests. All specimens were consolidated to the same nominal consolidation stresses, namely 200 kPa axial effective stress, σ'_{ac} and 90 kPa radial effective stress, σ'_{rc} resulting in a shear stress at end of consolidation τ_0 of 55 kPa. Consolidation was carried out by first increasing the cell pressure to σ'_{rc}, then applying dead weights in stages up to the final value of effective axial stress. The consolidation stage took in general about 1 hour. After consolidation, the specimens where left to stabilize overnight.

Five out of the six specimens were then subjected to drained cyclic preshearing, according to Table 2. Cyclic loading was carried out under axial load control, while keeping constant cell pressure. 400 cycles with sinusoidal constant-amplitude axial load, 10 seconds load period and continuous drainage were applied. The average shear stress during cycling, τ_{av} was specified equal to the consolidation shear stress in all tests, giving a normalized average shear stress ratio τ_{av}/σ'_{ac} of 0.28. The normalized cyclic shear stress $\tau_{cy\_pre}/\sigma'_{ac}$ was varied among the tests between 0.06 and 0.43 as detailed in Table 2. The cyclic preshearing stage lasted about 1 hour.

Finally, all specimens were sheared to failure under undrained cyclic loading. Loading was controlled in the same way as done in the preshearing stage. Drainage was prevented by closing the valve to the backpressure system. All specimens were sheared to failure under the same loading conditions, see Table 2.

Axial specimen deformations were measured in all stages using an external LVDT with a resolution of 0.002 mm (≈ 0.002% axial strain). Volume changes during consolidation were measured with a burette to the nearest 0.1 ml (≈ 0.04% volumetric strain). An external load cell was used to measure the load during cyclic stages of the tests.

3 RESULTS AND DISCUSSION

3.1 *Drained cyclic preshearing*

Figures 1a and 1b show the development of cyclic and permanent axial strains during cyclic preshearing, respectively. In all tests, the cyclic axial strain developed in the first cycle remains essentially constant as cyclic loading progresses. On the other hand, permanent axial strains gradually accumulate with increasing number of cycles. The rate of accumulation however markedly decreases in the first 50-100 cycles, i.e. the change in permanent axial strain from one cycle to the next becomes smaller and smaller as the number of cycles increases from the first one up to 50-100 cycles. This indicates that the specimens become stiffer with respect to development of permanent axial strains. This phenomenon is most evident for three tests with highest $\tau_{cy\_pre}/\sigma'_{ac}$ values (test ID CP-75-3, CP-75-4, CP-75-5).

Table 2. Laboratory program.

Test ID	Build-in	Drained cyclic preshearing			Undrained cyclic shear to failure	
-	Dr_i	N	τ_{av}/σ'_{ac}	$\tau_{cy\_pre}/\sigma'_{ac}$	τ_{av}/σ'_{ac}	τ_{cy}/σ'_{ac}
-	(%)	(-)	(-)	(-)	(-)	(-)
C-75-1	75.6	NA	NA	NA	0.28	0.50
CP-75-1	73.2	400	0.28	0.06	0.28	0.50
CP-75-2	77.2	400	0.28	0.12	0.28	0.50
CP-75-3	75.4	400	0.28	0.20	0.28	0.50
CP-75-4	75.5	400	0.28	0.30	0.28	0.50
CP-75-5	75.6	400	0.28	0.43	0.28	0.50

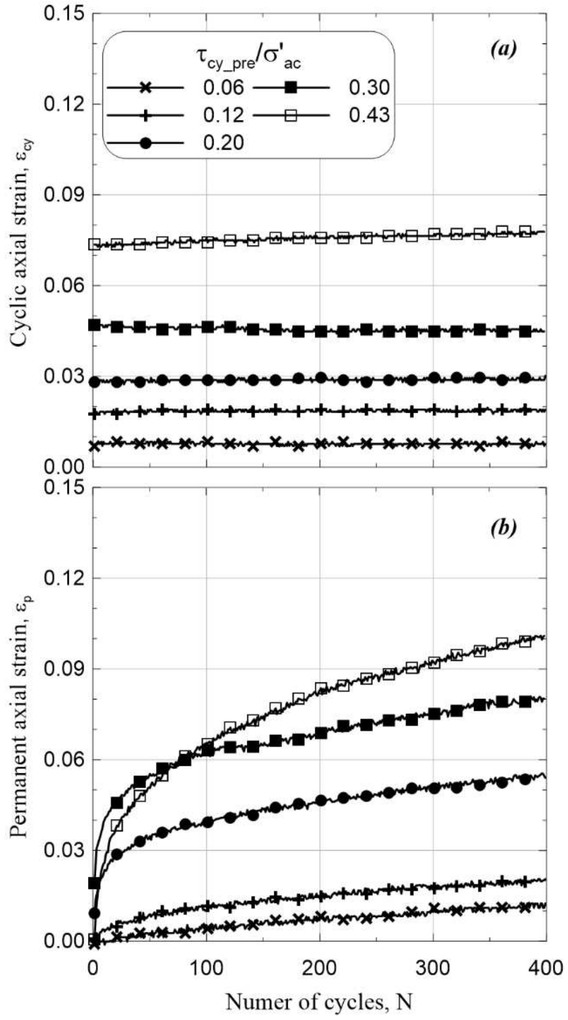

Figure 1. Drained cyclic preshearing phase. (a) Number of cycles versus cyclic axial strain and, (b) permanent axial strain

Figure 2 shows cyclic and permanent axial strains and permanent volumetric strains at the end of preshearing (N=400), as a function of $\tau_{cy\_pre}/\sigma'_{ac}$. Strains at the end of preshearing show an approximate linear increase with normalized cyclic shear stress. Permanent volumetric strains are calculated from measured permanent axial strains, assuming a ratio between radial and axial strain of 0.3. Permanent volumetric strain at end of preshearing was also checked using visual readings of the burette back pressure system for the tests with the smallest and largest $\tau_{cy\_pre}/\sigma'_{ac}$ values, namely test CP-75-1 and CP-75-5. The burette had a resolution of 0.1 ml, corresponding to 0.04% volumetric strains. Volume changes in the two tests were 0 ml and 0.1 ml, corresponding therefore to 0% and 0.04% increase in volumetric strain due to preshearing for CP-75-1 and CP-75-5, respectively. Given the resolution of the burette, the readings support the values of volumetric strains calculated from axial strains and assumed radial strains.

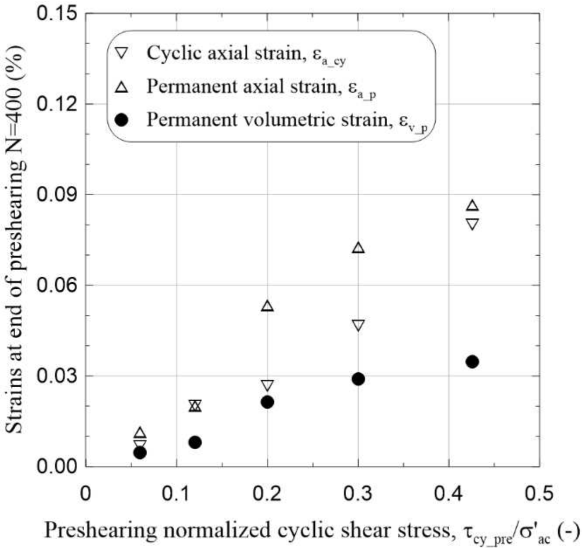

Figure 2. Drained preshearing phase. Normalized cyclic shear stress versus strains at end of preshearing (N = 400)

Relative densities at the end of preshearing, Dr_p are presented for each test in Table 3. Values at mounting and at end of consolidation, Dr_c are also reported, together with the relative density changes due to consolidation and to preshearing, ΔDr_c and ΔDr_p respectively. Relative densities at end of preshearing are calculated from the volumetric strains presented in Figure 2. The change in relative density occurring during preshearing is between 0.0% and 0.2%. The change in relative density due to consolidation is in comparison between 0.6% and 1.2%.

Table 3. Relative densities at mounting, end of consolidation and end of preshearing, including changes in relative densities due to consolidation and due to preshearing

Test	Dr_i	Dr_c	Dr_p	ΔDr_c	ΔDr_p
-	(%)	(%)	(%)	(%)	(%)
C-75-1	75.6	76.4	NA	0.8	NA
CP-75-1	73.2	74.2	74.2	1.0	0.0
CP-75-2	77.2	78.2	78.3	1.0	0.0
CP-75-3	75.4	76.6	76.7	1.2	0.1
CP-75-4	75.5	76.1	76.3	0.6	0.2
CP-75-5	75.6	76.4	76.6	0.8	0.2

3.1 *Undrained cyclic shearing to failure*

Upon completion of the drained cyclic preshearing phase, all specimens were sheared to failure under undrained conditions and identical cyclic loading.

Figure 3 shows the results of the undrained phase for the various tests in term of cyclic shear strain, γ_{cy} cyclic shear modulus, $G_{cy} = \tau_{cy}/\gamma_{cy}$ and normalized permanent pore pressure, u_p/σ'_{ac} presented versus number of cycles, N. All specimens failed due to sudden development of cyclic shear strains as soon as the latter exceeded typically 10%. In all tests G_{cy} consistently decreases with number of cycles and u_p/σ'_{ac} increases with number of cycles, until reaching a plateau around 0.28. This value corresponds to the state where the stress path has reached the failure line on the compression side. Compared to the specimen without preshearing, the specimens with $\tau_{cy\_pre}/\sigma'_{ac}$ equal to 0.20, 0.30 and 0.43 show systematically higher values of number of cycles to failure, N_f (Figure 3a) and of cyclic shear moduli at a given cycle (Figure 3b), and systematically lower values of normalized permanent pore pressure at a given cycle (Figure 3c). As an example, G_{cy} = 82 MPa at N = 1 for the test with $\tau_{cy\_pre}/\sigma'_{ac} = 0.43$, against G_{cy} = 45 MPa for the test without preshearing. At N = 30, the test without preshearing has reached the maximum value of u_p/σ'_{ac} and shows G_{cy} = 8 MPa, whereas the test with $\tau_{cy\_pre}/\sigma'_{ac} = 0.43$ has developed small u_p/σ'_{ac} values and G_{cy} is equal to 76 MPa, close to the value at N =1. On the other hand, the specimen with $\tau_{cy\_pre}/\sigma'_{ac}$ equal to 0.06% shows lower N_f and G_{cy} and higher u_p/σ'_{ac} compared to the test without preshearing. The specimen with $\tau_{cy\_pre}/\sigma'_{ac}$ equal to 0.12 behaves very similarly to the specimen without preshearing.

The effect of cyclic preshearing amplitude on the development of cyclic shear strain during the undrained phase can be directly compared in Figure 4. The figure presents the number of cycles to reach γ_{cy} = 0.5%, 1.0%, 5.0%, 10.0% and 15.0%, plotted as a function of $\tau_{cy\_pre}/\sigma'_{ac}$ applied in each test. The number of cycles to a given cyclic strain is virtually unaffected by preshearing amplitude up to $\tau_{cy\_pre}/\sigma'_{ac} = 0.12$, whereas it is significantly affected at higher values of $\tau_{cy\_pre}/\sigma'_{ac}$, increasing approximately linearly with $\tau_{cy\_pre}/\sigma'_{ac}$; As an example, the number of cycles to γ_{cy} = 15.0% (also number of cycles to failure) is 245 for the test with $\tau_{cy\_pre}/\sigma'_{ac} = 0.43$ and 60 for the test without preshearing, giving a factor of 4.1 between the two cases. However, by observing that the lines for the different cyclic strain values in Figure 4 plot parallel to each other, it can be further noted that it is the number of cycles required to reach γ_{cy} = 0.5% which is significantly dependent on cyclic preshearing amplitude (for $\tau_{cy\_pre}/\sigma'_{ac} > 0.12$) whereas the number of cycles required to progress from γ_{cy} = 0.5% up to γ_{cy} = 15.0% is independent on cyclic preshearing amplitude. The data therefore indicate that the specimen "remembers" the effect previous cyclic preloading until $\gamma_{cy} <= 0.5\%$; after this point the effect is erased and the specimen progress to failure independently of previous cyclic preshearing. Moreover, the effect of previous cyclic preshearing is significant for $\tau_{cy\_pre}/\sigma'_{ac} > 0.12$, whereas it is marginal below this value.

To further investigate the effect of cyclic preshearing amplitude, the relationship between cyclic shear strains and normalized permanent pore pressures during undrained shearing is shown in Figure 5. In this figure, γ_{cy} is plotted against the normalized permanent pore pressure ratio, u_{nor} defined as the ratio $(u_p/\sigma'_{ac})/(u_p/\sigma'_{ac})_{max}$, where $(u_p/\sigma'_{ac})_{max}$ is the maximum value of u_p/σ'_{ac} within the test. The figure shows that the data for the different tests plot in a narrow band, with some minor deviations. This indicates that the relationship between γ_{cy} and u_{nor} is independent of number of cycles and is a function of the average and cyclic effective shear stress components. Moreover, it is observed that the value γ_{cy} = 0.5% corresponds to a small range of u_{nor} between 0.87 and 0.95 for all test, i.e. γ_{cy} = 0.5% is reached when about 90% of the maximum permanent pore pressure is mobilized. Building upon the observation from Figure 4, it can therefore be concluded that cyclic preshearing larger than 0.12 significantly increases the number of cycles required to mobilize about 90% of the maximum permanent pore pressure, and that the "history" from cyclic preshearing is erased above this value.

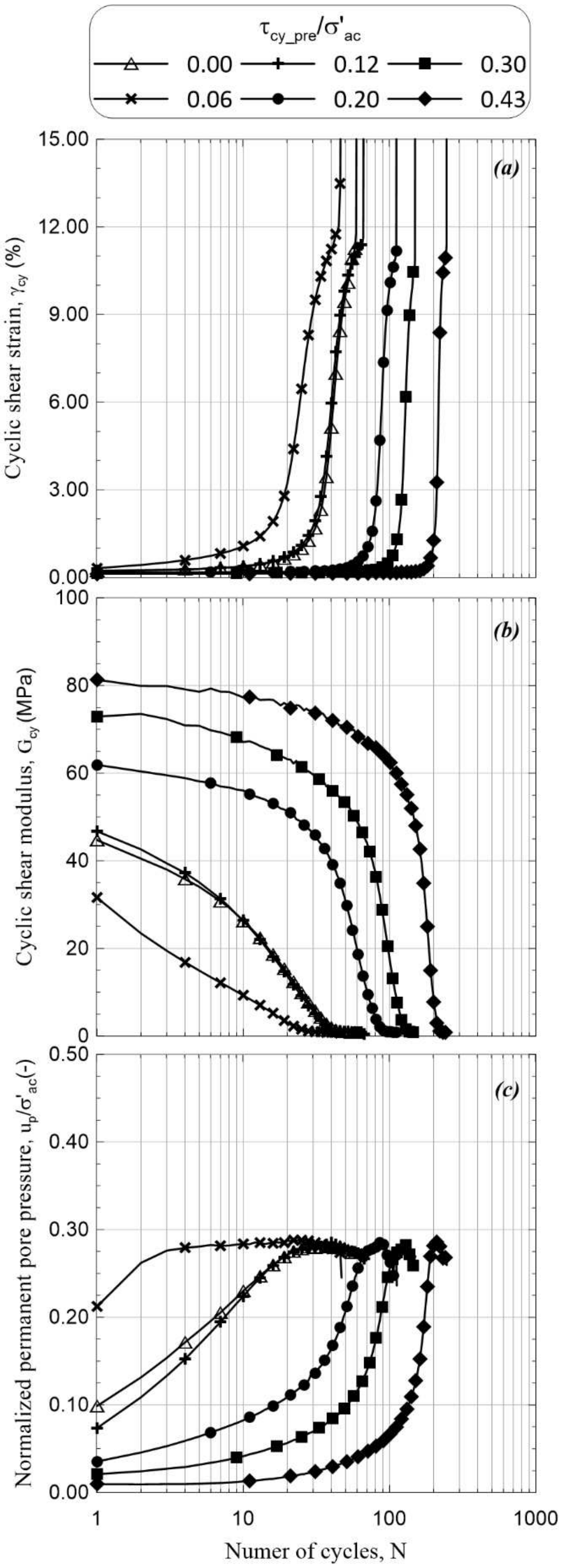

Figure 3. Undrained shearing to failure phase. Number of cycles versus cyclic shear strain (a), cyclic shear modulus (b) and normalized permanent pore pressure (c), for different normalized cyclic shear stresses during preshearing

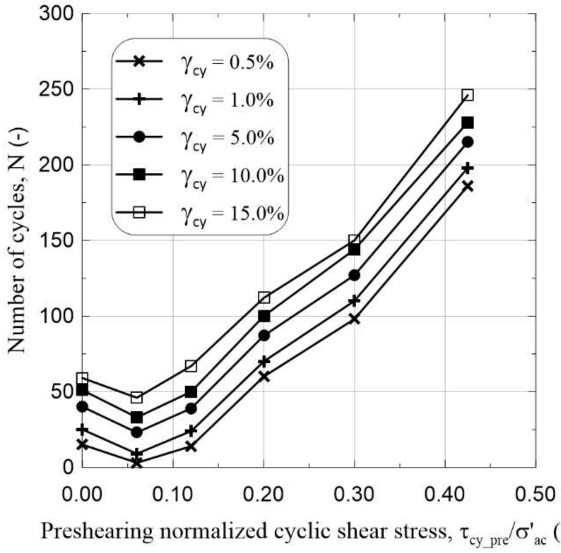

Figure 4. Normalized cyclic shear stress during preshearing versus number of cycles at various levels of cyclic shear strain during undrained shearing to failure

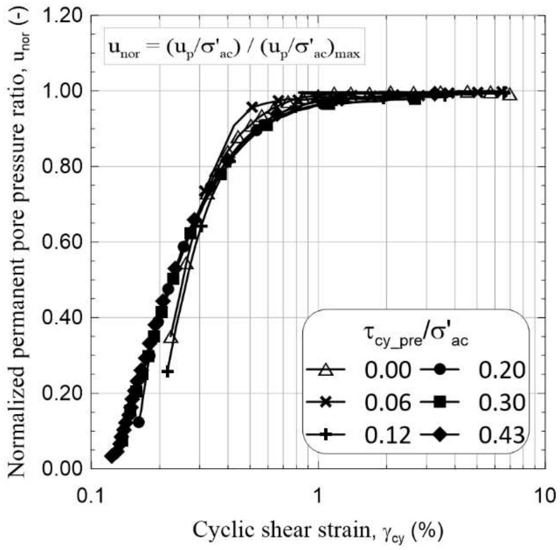

Figure 5. Undrained shearing to failure phase. Cyclic shear strain versus normalized permanent pore pressure ratio for different normalized cyclic shear stress during cyclic preshearing

3.3 *Discussion*

Based on the experimental results and analyses of the undrained cyclic shearing phase it is observed that: (a) drained cyclic preshearing for $\tau_{cy\_pre}/\sigma'_{ac} > 0.12$ provides a memory to the specimen so that the number of cycles required to mobilize 90% of the maximum normalized permanent pore pressure significantly increases with $\tau_{cy\_pre}/\sigma'_{ac}$, and (b) this memory is erased beyond this 90% threshold, so that the additional number of cycles required to reach failure is independent of $\tau_{cy\_pre}/\sigma'_{ac}$. As a consequence, G_{cy} and number of cycles to failure significantly increase as $\tau_{cy\_pre}/\sigma'_{ac}$ increases. The 90% threshold is found to coincide with γ_{cy} of about 0.5%.

The response described above is consistent with the increase is specimen stiffness during preshearing observed in Figure 1b. In fact, it was noted that for the tests with $\tau_{cy\_pre}/\sigma'_{ac} > 0.12$, the rate of accumulation of permanent axial strain markedly decreases in the first 50-100 cycles, indicating that the specimens are becoming stiffer as drained cyclic preshearing progress. Consistently, the tests with $\tau_{cy\_pre}/\sigma'_{ac} > 0.12$ show a stiffer response also in the subsequent undrained cyclic loading.

The change in relative density occurring during drained cyclic preshearing does not reflect the response under undrained shearing. In fact, it was observed that the maximum change in relative density due to preshearing is 0.2%. This value is considered insignificant for practical purposes: two specimens reconstituted and tested in the same way except for a 0.2% difference in initial relative density, would not be expected to show any systematic difference in shearing behavior.

Having excluded the change in Dr as the cause of the observed results, the hypothesis proposed is that drained cyclic preshearing causes a re-arrangement of intergranular reactions. It may be argued that this reaction re-arrangement provides the specimen with a more stable structure, increasing its stiffness both during the drained cyclic preshearing (Figure 1b) and in the following undrained cyclic shearing to failure (Figures 3 and 4). As the specimen reaches high values of normalized permanent pore pressure ratios, here identified with a threshold of 90%, its stress path approaches the failure line. It is reasonable to assume that as the failure line is approached, the stable structure of intergranular reactions imprinted by cyclic drained preshearing is broken down and the soil response becomes controlled by the overall relative density. This is consistent with the observation in the tests that after 90% of maximum normalized permanent pore pressure is developed, the additional number of cycles required to reach failure is independent of the preshearing cyclic shear amplitude (Figure 4). The data suggest that $\tau_{cy\_pre}/\sigma'_{ac}$ values above 0.12 are necessary to develop an intergranular reaction re-arrangement that makes a significant impact on the sand response. For smaller values of $\tau_{cy\_pre}/\sigma'_{ac}$, encompassing the typical range 0.04-0.06 applied in offshore practice, intergranular reaction re-arrangement does not seem to have a significant impact. This might explain why previous researchers (e.g. Quinteros et al. 2017) have found little preshearing effects in their tests.

The hypothesis presented opens for some interesting considerations. As many offshore sand deposits have undergone wave loading for thousands of years, it can be assumed that they have acquired the most stable possible configuration of intergranular reactions. In the light of the tests presented, it can be postulated that the intergranular reaction configuration generated by drained cyclic preshearing is more representative of in-situ conditions than the intergranular reaction configuration resulting directly from moist-tamping reconstitution. This postulate could be tested by comparing the existing data set with future tests on undisturbed specimens from the same sand, potentially recovered by soil freezing. It can be further speculated that the difference in sand response observed by different reconstitution methods (e.g. Knudsen et al. 2019) may be reduced when specimens undergo drained cyclic preshearing with large $\tau_{cy\_pre}/\sigma'_{ac}$ values, up to 0.3-0.4: the intergranular reaction configuration might converge towards a unique state for the different methods. This suggestion could be checked by parallel testing with different reconstitution methods.

It is underlined that the results in this paper are limited to clean dense silica sands. Loose sands, sands with not-plastic or plastic fines, not-silica sands, locked or cemented sands, might show different behavior than that found in this series of tests. Moreover, the testing program is limited to a narrow range of consolidation stresses and undrained cyclic loading stresses.

4 CONCLUSIONS

In order to investigate the effect of drained cyclic load history (*preshearing*) on the subsequent undrained cyclic response to failure of a clean dense silica sand in the triaxial apparatus, the results of a series of undrained cyclic triaxial tests is presented and discussed.

The experimental results show that for preshearing with normalized cyclic shear stress $\tau_{cy\_pre}/\sigma'_{ac}$ higher than 0.12:

(a) a memory of the load history is given to the specimen so that the number of cycles required to mobilize 90% of the maximum normalized permanent pore pressure during undrained cyclic loading to failure significantly increases as $\tau_{cy\_pre}/\sigma'_{ac}$ increases;

(b) this memory is erased beyond this 90% threshold, so that the additional number of cycles required to reach failure is independent of $\tau_{cy\_pre}/\sigma'_{ac}$; The 90% threshold is found to coincide with γ_{cy} of about 0.5%.

(c) the combination points (a) and (b) gives a significant increase of both N_f and G_{cy} during undrained cyclic loading as $\tau_{cy\_pre}/\sigma'_{ac}$ increases, whereas a significant decrease in normalized permanent pore pressure. As an example, G_{cy} ranges between 82 MPa and 76 MPa in the first 30 cycles and N_f is 245 for the test with highest preshearing amplitude. For the test without preshearing G_{cy} is between 45 MPa and 8 MPa in the first 30 cycles and N_f is equal to 60.

(d) the cause of this behavior is not the change in relative density during cyclic preshearing, since this change is small (maximum 0.2%)

It is speculated that the behavior described above is due to a re-arrangement of intergranular reactions occurring during cyclic preshearing, which provides the specimen with a more stable intergranular structure compared to the initial one given by moist tamping. As the specimen reaches 90% of maximum normalized permanent pore pressure, its stress path approaches the failure line and the original stable structure of intergranular reactions is broken down and the soil response becomes controlled by the overall relative density. This hypothesis is found also to be consistent with the observed increase in stiffness during cyclic preshearing. It is further found that for normalized cyclic shear stress less than or equal to 0.12, the impact of preshearing is small to negligible. This might indicate that intergranular reaction re-arrangement is minor or does not occur for these small values of preshearing amplitudes.

It is proposed that the intergranular reaction re-arrangement given by high values of preshearing is more representative of in-situ conditions of old dense silica sands than the intergranular reaction arrangement resulting directly from moist-tamping reconstitution in the laboratory. If this is the case, it would imply that much higher cyclic stiffness and strength could be used in design.

5 ACKNOWLEDGEMENTS

The Norwegian Research Counsil (NFR) financed this testing program through NGI basic funding. This support is much appreciated. The author would thank many NGI colleagues who helped with useful discussion, and NGI workshop that is always available to provide assistance with laboratory equipment.

6 REFERENCES

Andersen, K. H. (2015). “Cyclic soil parameters for offshore foundation design.” Frontiers in Offshore Geotechnics III - Proceedings of the 3rd International Symposium on Frontiers in Offshore Geotechnics, ISFOG 2015, 82.

Ladd, R. S. (1978). “Preparing test specimens using undercompaction.” Geotechnical Testing Journal, GTJODJ, 1(1), 16–23.

Knudsen, S., Lunne, T., Quinteros, V. S., Vestgården, T., Krogh, L., and Bøgelund-Pedersen, R. (2019). “Effect of reconstitution techniques on the triaxial stress-strength behaviour of a very dense sand" Proceedings of the XVII ECSMGE-2019, Geotechnical Engineering foundation of the future.

Quinteros, V., Lunne, T., Dyvik, R., Krogh, L., Bøgelund-Pedersen, R., and Bøtker-Rasmussen, S. (2017). “Influence of Pre-Shearing on the Triaxial Drained Strength and Stiffness of a Marine North Sea Sand.” Offshore Site Investigation Geotechnics 8th International Conference Proceedings, 338–345.

Seed, H. B., Mori, K., and Chan, C. K. (1977). "Influence of seismic history on liquefaction of sands." Journal of geotechnical engineering division, 103(4), 257–270.